Pattern formations in fluids and computer assisted analysis

Takaaki Nishida *

Abstract. Pattern formations from the equilibrium state in fluid motions may be treated by the bifurcation theories. Bifurcation theorems can be applied to explain Taylor vortices of Taylor problems and hexagonal cells of heat convection problems as the first bifurcation. Computer assisted analysis becomes necessary to see global bifurcation structures. In this lecture examples of computer assisted proofs and analysis are explained for some heat convection problems.

1 Examples of pattern formations in fluids

1.1

Bénard observed that fluid in a plane heated from below develops a regular pattern of convection cells, above a certain threshold of temperature. The cell pattern is roughly classified into the roll-type, rectangle-type and hexagon-type. Rayleigh first analyzed the pattern formation theoretically.

Taylor showed theoretically that fluid in the gap between two rotating cylinders on the same axis develops axisymmetric toroidal vortices, above a certain threshold in angular velocity of the cylinders.

Kármán studied that a flow of fluid past a rigid body develops swirling vortices, above a certain threshold in velocity of the flow.

1.2

We focus our attention on the heat convection problems. Let us consider the general equation of motion of compressible fluid with viscosity and thermal conductivity in terms of Bénard's experiment. For any difference ΔT between the temperature of the lower and upper boundaries, we have the (trivial) heat conduction solutions which correspond to the motionless state of the fluid. It is expected that, above a certain threshold of ΔT, the heat conduction solutions get unstable and nontrivial solutions appear which may be stable and correspond to the cell patterns mentioned above. The main tool for

*Department of Pure and applied Mathematics, Waseda University, Tokyo 169-8555, Japan. Supported in part by JSPS Kakenhi No. 20540141 and by Japan-Germany joint project on Mathematical Fluid Dynamics.

mathematical analysis is the bifurcation theory. However the general equation of the fluid is so complicated that the above scenario has not yet been justified.

We introduce a simplified equation called the Oberbeck-Boussinesq equation, which is believed to approximate the original equation. (Note that the approximation is not justified mathematically.) The dimensionless Oberbeck-Boussinesq equation is given as follows:

$$\text{(1.1)} \qquad \begin{cases} \dfrac{1}{\mathcal{P}_r}\Big(\dfrac{\partial \vec{u}}{\partial t} + \vec{u}\cdot\nabla\vec{u}\Big) + \nabla p = \Delta\vec{u} - \rho(T)\nabla z, \\ \nabla\cdot\vec{u} = 0, \\ \dfrac{\partial T}{\partial t} + \vec{u}\cdot\nabla T = \Delta T, \end{cases}$$

where $\vec{u}(t,x,y,z), p(t,x,y,z), T(t,x,y,z)$ are unknown velocity, pressure, temperature,

$$\rho(T) := G - \mathcal{R}_a T$$

is density assumed to depends only on gravity and buoyancy (the Oberbeck-Boussinesq approximation), $\mathcal{P}_r$ is the Prandtl number, $\mathcal{R}_a$ is the Rayleigh number and G is the gravity constant. We consider (1.1) in the horizontal strip $\{x \in \mathbb{R}, y \in \mathbb{R}, z \in (0,1)\}$ with the boundary condition $T(0) = 1$, $T(1) = 0$. This normalization reflects $\mathcal{R}_a$. The parameter $\mathcal{R}_a$ is a bifurcation parameter of our problem. The (trivial) solutions which correspond to the equilibrium state, or the heat conductive state are given for all $\mathcal{P}_r > 0$ and $\mathcal{R}_a > 0$ by

$$U_e = (\vec{u}_e, T_e, p_e) = \left(0,\, 1-z,\, G(1-z) - \mathcal{R}_a\Big(\frac{1}{2} - z + \frac{z^2}{2}\Big) + p_a\right),$$

where p_a is the pressure of the atmosphere.

Our purpose is to investigate the bifurcation from U_e. Let us consider solutions of (1.1) of the form $U_e + (\vec{u}, \theta, p)$. We study the evolution of $(\vec{u}, \theta, p)$ in order to find the critical Rayleigh number at which the stability of U_e changes from stable to unstable. The equation of $(\vec{u}, \theta, p)$, $\vec{u} = (u, v, w)$ is given by

$$\text{(1.2)} \qquad \begin{cases} \dfrac{1}{\mathcal{P}_r}\Big(\dfrac{\partial \vec{u}}{\partial t} + \vec{u}\cdot\nabla\vec{u}\Big) + \nabla p = \Delta\vec{u} + \mathcal{R}_a\theta\nabla z, \\ \dfrac{\partial \theta}{\partial t} + \vec{u}\cdot\nabla\theta = \Delta\theta + w, \\ \nabla\cdot\vec{u} = 0. \end{cases}$$

For simplicity we impose the periodic boundary conditions with respect to x and y, namely we consider (1.2) in $\{x \in [0, 2\pi/a],\ y \in [0, 2\pi/b],\ z \in (0,1)\}$ with the periodicity in x, y. There are several types of boundary conditions with respect to z.

1. The stress free boundary conditions:

$$\frac{\partial u}{\partial z}\Big|_{z=0,1} = 0, \quad \frac{\partial v}{\partial z}\Big|_{z=0,1} = 0, \quad w|_{z=0,1} = 0, \quad \theta|_{z=0,1} = 0.$$

2. The stress free boundary condition on the upper boundary and the fixed boundary condition on the lower boundary:

   For $z = 1$ it is the same as 1. $u|_{z=0} = 0, \quad v|_{z=0} = 0, \quad w|_{z=0} = 0, \quad \theta|_{z=0} = 0.$

3. The free surface $\eta(t, x, y)$ on the upper boundary and the fixed boundary condition on the lower boundary:

   η is determined by the surface tension effects. For $z = 0$, it is the same as 2.

2. and 3. are more natural than 1. The problem (1.2) with 1. is called the "Rayleigh-Benard problem" and (1.2) with 3. the "Benard-Marangoni problem".

1.3

Now we review the results of the case 1, which was studied by Rayleigh in 1916. In order to obtain simple eigen values, we suppose the following even or odd properties:

$$\begin{aligned}
&u(x,y,z) = -u(-x,y,z) = u(x,-y,z), \;\; v(x,y,z) = v(-x,y,z) = -v(x,-y,z),\\
&w(x,y,z) = w(-x,y,z) = w(x,-y,z), \;\; \theta(x,y,z) = \theta(-x,y,z) = \theta(x,-y,z),\\
&p(x,y,z) = p(-x,y,z) = p(x,-y,z).
\end{aligned}$$

We look for solutions which can be expanded into Fourier series:

$$\text{(1.3)} \qquad \begin{cases}
u(t,x,y,z) = \displaystyle\sum_{l,m,n} u_{lmn}(t)\sin(alx)\cos(bmy)\cos(n\pi z),\\
v(t,x,y,z) = \displaystyle\sum_{l,m,n} v_{lmn}(t)\cos(alx)\sin(bmy)\cos(n\pi z),\\
w(t,x,y,z) = \displaystyle\sum_{l,m,n} w_{lmn}(t)\cos(alx)\cos(bmy)\sin(n\pi z),\\
\theta(t,x,y,z) = \displaystyle\sum_{l,m,n} \theta_{lmn}(t)\cos(alx)\cos(bmy)\sin(n\pi z),\\
p(t,x,y,z) = \displaystyle\sum_{l,m,n} p_{lmn}(t)\cos(alx)\cos(bmy)\cos(n\pi z).
\end{cases}$$

We call the lmn-element of (1.3) "(l, m, n)-mode". The linearized equation of (1.2) around the trivial solution 0 is given by

$$\text{(1.4)} \qquad \begin{cases}
\dfrac{\partial \vec{u}}{\partial t} + \mathcal{P}_r \nabla p = \mathcal{P}_r \Delta \vec{u} + \mathcal{P}_r \mathcal{R}_a \theta \nabla z,\\[2ex]
\dfrac{\partial \theta}{\partial t} = \Delta\theta + w,\\[2ex]
\nabla \cdot \vec{u} = 0.
\end{cases}$$

We rewrite (1.4) as $\mathcal{M}\frac{\partial U}{\partial t} = -\mathcal{L}U$, where

$$U := \begin{bmatrix} u \\ v \\ w \\ \theta \\ p \end{bmatrix}, \quad \mathcal{M} := \begin{bmatrix} 1 & 0 & 0 & 0 & 0 \\ 0 & 1 & 0 & 0 & 0 \\ 0 & 0 & 1 & 0 & 0 \\ 0 & 0 & 0 & 1 & 0 \\ 0 & 0 & 0 & 0 & 0 \end{bmatrix},$$

$$\mathcal{L} := \begin{bmatrix} -\mathcal{P}_r\Delta & 0 & 0 & 0 & -\mathcal{P}_r\frac{\partial}{\partial x} \\ 0 & -\mathcal{P}_r\Delta & 0 & 0 & -\mathcal{P}_r\frac{\partial}{\partial y} \\ 0 & 0 & -\mathcal{P}_r\Delta & -\mathcal{P}_r\mathcal{R}_a & -\mathcal{P}_r\frac{\partial}{\partial z} \\ 0 & 0 & -1 & -\Delta & 0 \\ -\mathcal{P}_r\frac{\partial}{\partial x} & -\mathcal{P}_r\frac{\partial}{\partial y} & -\mathcal{P}_r\frac{\partial}{\partial z} & 0 & 0 \end{bmatrix}.$$

Inserting (1.3) into the linearized equation, we have the ODE for each fixed l, m, n

$$\mathcal{M}U'_{lmn}(t) = -\mathcal{L}_{lmn}U_{lmn}(t), \tag{1.5}$$

where

$$U_{lmn}(t) := \begin{bmatrix} u_{lmn}(t) \\ v_{lmn}(t) \\ w_{lmn}(t) \\ \theta_{lmn}(t) \\ p_{lmn}(t) \end{bmatrix}, \quad \mathcal{L}_{lmn} := \begin{bmatrix} \mathcal{P}_r A_{lmn}^2 & 0 & 0 & 0 & -\mathcal{P}_r al \\ 0 & \mathcal{P}_r A_{lmn}^2 & 0 & 0 & -\mathcal{P}_r bm \\ 0 & 0 & \mathcal{P}_r A_{lmn}^2 & -\mathcal{P}_r\mathcal{R}_a & -\mathcal{P}_r\pi n \\ 0 & 0 & -1 & A_{lmn}^2 & 0 \\ -\mathcal{P}_r al & -\mathcal{P}_r bm & -\mathcal{P}_r\pi n & 0 & 0 \end{bmatrix}$$

with $A_{lmn}^2 := (al)^2 + (bm)^2 + (\pi n)^2$. We remark that (1.5) is not a usual first order differential equation ($\mathcal{M}$ is degenerate). We can get solutions of (1.5) of the form

$$U_{lmn}(t) = e^{t\lambda_{lmn}}U_{lmn}(0),$$

if λ_{lmn} and $U_{lmn}(0)$ satisfy the following eigen value problem:

$$\left\{\lambda_{lmn}\mathcal{M} + \mathcal{L}_{lmn}\right\}U_{lmn}(0) = 0. \tag{1.6}$$

Therefore we obtain solutions of (1.4) with exponential evolution in time. The linear stability of the trivial solution 0 of (1.2), which means the linear stability of U_e, is determined by the sign of λ_{lmn}. (1.6) yields the real eigen values for any $\mathcal{P}_r, \mathcal{R}_a > 0$

$$\begin{aligned} \lambda_{lmn}^0 &= -\mathcal{P}_r A_{lmn}^2, \\ \lambda_{lmn}^{\pm} &= -\frac{1}{2}(1+\mathcal{P}_r)A_{lmn}^2 \pm \frac{1}{2}\sqrt{(1+\mathcal{P}_r)^2 A_{lmn}^4 + 4\mathcal{P}_r\frac{\{(al)^2+(bm)^2\}\mathcal{R}_a - A_{lmn}^6}{A_{lmn}^2}}. \end{aligned}$$

λ_{lmn}^0,λ_{lmn}^- are always negative and λ_{lmn}^+ changes its sign from negative into positive at

$$\mathcal{R}_a = \frac{\{(al)^2 + (bm)^2 + (\pi n)^2\}^3}{(al)^2 + (bm)^2}.$$

For each fixed aspect a, b all the modes has negative eigenvalues, if $\mathcal{R}_a$ satisfies

$$\mathcal{R}_a < \mathcal{R}_{ac}(a,b) := \inf_{l,m,n} \frac{\{(al)^2 + (bm)^2 + (\pi n)^2\}^3}{(al)^2 + (bm)^2}.$$

If $\mathcal{R}_a < \mathcal{R}_{ac}(a,b)$, the trivial solution 0 of (1.2), and therefore the heat conductive solution U_e, are linear stable. Hence U_e is locally nonlinear stable. Joseph proved with the energy method and a variational technique that, if $\mathcal{R}_a < \mathcal{R}_{ac}(a,b)$, U_e is globally nonlinear stable. If $\mathcal{R}_a > \mathcal{R}_{ac}(a,b)$, the trivial solution 0 of (1.2), and therefore U_e are linearly unstable. In this case it is expected that the original nonlinear problem has

another (non-trivial) stable solution. We prove this by bifurcation theories. We conclude this section with the following remark:

(1) $\inf_{a,b} \mathcal{R}_{ac}(a,b) = 6.75 \times \pi^4$.

(2) $\mathcal{R}_{ac}(\frac{1}{2\sqrt{2}}, \sqrt{3}a) = 6.75 \times \pi^4$ for $(l,m,n) = (2,0,1)$ and $(1,1,1)$.

(3) If $a = \frac{1}{2\sqrt{2}}$ and $b = \sqrt{3}a$, the linear stability of U_e changes from stable into unstable at $\mathcal{R}_a = 6.75 \times \pi^4$ from the $(2,0,1)$-mode and $(1,1,1)$-mode.

2 Bifurcation theories

2.1

We want to find non-trivial solutions of an equation $F(u,\gamma) = 0$ depending on a parameter γ, which is the stationary problem of $\frac{\partial u}{\partial t} + F(u,\gamma) = 0$. We may or may not have the non-trivial solutions, according to γ. The useful tool for this argument is bifurcation theorems. Now we state the simple stationary bifurcation theorem.

Theorem (Crandall-Rabinowitz). *Let X, Y be Banach spaces and $O \subset X$ is a neighborhood of $0 \in X$. Let $F(u,\gamma) : O \times (-1,1) \to Y$ be a twice continuously differentiable mapping which satisfies $F(0,\gamma) = 0$ for all $\gamma \in (-1,1)$. Suppose that*

(A1) $\mathcal{N}\big(D_uF(0,0)\big) := \{u \in X \,|\, D_uF(0,0)u = 0\}$ is one-dimensional and spanned by u_0,

(A2) $\mathcal{R}\big(D_uF(0,0)\big) := \{D_uF(0,0)u \,|\, u \in X\}$ has co-dimension 1, i.e. $Y \backslash \mathcal{R}\big(D_uF(0,0)\big)$ is one-dimensional,

(A3) $D_{u\gamma}F(0,0)u_0 \notin \mathcal{R}\big(D_uF(0,0)\big)$,

where D_uF, etc. stand for the Fréchet derivatives of F. Then there exist a neighborhood W of $(0,0)$ contained in $O \times (-1,1)$ and a number $s_0 > 0$ for which we have C^1-mappings

$$u(s) = su_0 + s\varphi(s) : (-s_0, s_0) \to O, \quad \gamma(s) : (-s_0, s_0) \to (-1,1)$$

with $\varphi(s) \in X \setminus \mathcal{N}\big(D_uF(0,0)\big)$, $\varphi(0) = 0$ and $\gamma(0) = 0$ which yield the family of the non-trivial solutions of $F(u,\lambda) = 0$ in W, namely

$$F^{-1}(0) \cap W = \{(0,\gamma) \,|\, (0,\gamma) \in W\} \cup \{(u(s), \gamma(s) \,|\, s \in (-s_0, s_0))\}.$$

Idea of Proof. Basic idea is to use the implicit function theorem in Banach spaces. We introduce $f(s,\gamma,z) : B \times Z \to Y$, where $B \subset \mathbb{R}^2$ is a neighborhood of 0 and $Z := \big(X \setminus \mathcal{N}\big(D_uF(0,0)\big)\big) \cup \{0\}$, defined by

$$f(s,\gamma,z) = \begin{cases} \dfrac{1}{s}F(su_0 + sz, \gamma) & \text{for } s \neq 0 \\ \\ D_uF(0,\gamma)(u_0 + z) & \text{for } s = 0. \end{cases}$$

Note that f is C^1. Since u_0 spans $\mathcal{N}\big(D_uF(0,0)\big)$, we have

$$f(0,0,0) = D_uF(0,0)u_0 = 0.$$

If the implicit function theorem is applicable to f around $(0,0,0)$, we would obtain $\gamma(s), z(s)$ such that

$$0 \equiv f(s,\gamma(s),z(s)) = \frac{1}{s}F(su_0 + sz(s),\gamma(s)),$$

which leads to the substantial part of our purpose, namely

$$F^{-1}(0)\cap W \supset \{(0,\gamma)\,|\,(0,\gamma)\in W\}\cup\{(u(s),\gamma(s)\,|\,s\in(-s_0,s_0))\}.$$

In fact we can check the condition for the implicit function theorem: It is enough to show that $D_{(\gamma,z)}f(0,0,0):\mathbb{R}\times Z\to Y$ is homeomorphic. We observe that

$$D_{(\gamma,z)}f(0,0,0)(\gamma,z) = D_{u\gamma}F(0,0)u_0\gamma + D_uF(0,0)z$$

is continuous.

If $D_{(\gamma,z)}f(0,0,0)(\gamma,z)=0$, we have $D_{u\gamma}F(0,0)u_0\gamma = -D_uF(0,0)z \in \mathcal{R}\big(D_uF(0,0)\big)$. By (A3), γ must be 0. Hence $D_uF(0,0)z = 0$. Since $z\in Z\setminus\{0\}$ do not belong to $\mathcal{N}\big(D_uF(0,0)\big)$, z must be 0. Therefore $D_{(\gamma,z)}f(0,0,0)$ is one to one.

Let y be an arbitrary element of Y. We want to solve $D_{(\gamma,z)}f(0,0,0)(\gamma,z)=y$. It follows from (A2) and (A3) that

$$Y = \{D_{u\gamma}F(0,0)u_0t\,|\,t\in\mathbb{R}\}\oplus\mathcal{R}\big(D_uF(0,0)\big).$$

Hence we have $\gamma^*\in\mathbb{R}$ and $y_1\in\mathcal{R}(D_uF(0,0))$ such that $y=\gamma^*y_0+y_1$ with $y_0 = D_{u\gamma}F(0,0)u_0$. Since y_1 belongs to $\mathcal{R}\big(D_uF(0,0)\big)$, we have $u\in X$ such that $D_uF(0,0)u = y_1$. It follows from the definition of Z that

$$X = \{tu_0\,|\,t\in\mathbb{R}\}\oplus Z.$$

Hence we have $t^*\in\mathbb{R}$ and $z^*\in Z$ such that $u = t^*u_0 + z^*$. Therefore we obtain

$$\begin{aligned}
&D_uF(0,0)u = D_uF(0,0)z^* = y_1,\\
&D_{(\gamma,z)}f(0,0,0)(\gamma^*,z^*) = D_{u\gamma}F(0,0)u_0\gamma^* + D_uF(0,0)z^* = \gamma^*y_0 + y_1 = y,
\end{aligned}$$

which means that $D_{(\gamma,z)}f(0,0,0)$ is onto.

We can get

$$F^{-1}(0)\cap W \subset \{(0,\gamma)\,|\,(0,\gamma)\in W\}\cup\{(u(s),\gamma(s)\,|\,s\in(-s_0,s_0))\}$$

by estimating $\parallel su_0+z\parallel+|\gamma|$ for any solution (su_0+z,γ) of $F=0$ in W and using the uniqueness of the implicit function. □

2.2

We state the stability condition of bifurcated solutions. Let us consider

$$\begin{aligned} D_u F(0,\gamma)u(\gamma) &= \lambda(\gamma)u(\gamma), \quad \gamma \in I, \\ D_u F(u(s),\gamma(s))w(s) &= \mu(s)w(s), \quad s \in J. \end{aligned}$$

Note that the bifurcated solutions $u(s)$ is stable, if and only if $\mu(s) < 0$.

Theorem (Crandall-Rabinowitz). *The following holds:*

$$\frac{d\lambda}{d\gamma} \neq 0, \qquad \lim_{s\to 0, \mu(s)\neq 0} \frac{-s\frac{d\gamma}{ds}(s)\frac{d\lambda}{d\gamma}(0)}{\mu(s)} = 1.$$

Suppose that $\lambda(0) = 0$ and $\frac{d\lambda}{d\gamma}(0) > 0$. Then $\lambda(\gamma) < 0$ for $\gamma < 0$ and the trivial solution is stable ($\lambda(\gamma) > 0$ for $\gamma > 0$ and the trivial solution is unstable). Furthermore if we have

$$s\frac{d\gamma}{ds}(s) > 0,$$

then $\mu(s) < 0$ due to Theorem and the bifurcated solutions are stable. (see the left in Figure 1.) Similarly if we have

$$s\frac{d\gamma}{ds}(s) < 0,$$

then $\mu(s) > 0$ due to Theorem and the bifurcated solutions are unstable. (see the right in Figure 1.)

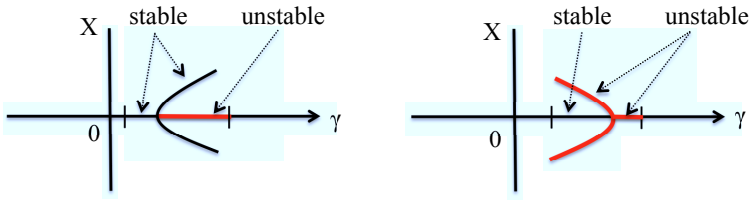

Figure 1.

3 Applications of bifurcation theorems

3.1

We apply the simple stationary bifurcation theorem to (1.2) with the stress free boundary conditions. Fix $\mathcal{P}_r$ and set $\gamma := \mathcal{R}_a - \mathcal{R}_{ac}$ with $\mathcal{R}_{ac} = 6.75 \times \pi^4$. The stationary problem of (1.2) is rewritten as

$$F(U,\gamma) = 0,$$

where $U = (u, v, w, \theta, p)$ is of the Fourier series (1.3) and $F : X \times \mathbb{R} \to Y$ with

$$\begin{aligned} X &= H^2_{a,b} := \{(u,v,w,\theta,p) \,|\, \sum_{l,m,n} \{((al)^2 + (bm)^2 + (\pi n)^2)^2 (u^2_{lmn} + v^2_{lmn} + w^2_{lmn} + \theta^2_{lmn}) \\ &\qquad + ((al)^2 + (bm)^2 + (\pi n)^2) p^2_{lmn} < \infty\}, \\ Y &= L^2_{a,b} := \{(u,v,w,\theta,p) \,|\, \sum_{l,m,n} (u^2_{lmn} + v^2_{lmn} + w^2_{lmn} + \theta^2_{lmn} + p^2_{lmn}) < \infty\}. \end{aligned}$$

We already know about the zero eigenvalue of the eigenvalue problem

$$D_U F(0,0)U = \lambda U$$

through the study of (1.6), where $D_u F(0,0) = \mathcal{L}$. Let (l_0, m_0, n_0)-mode be an eigenfunction of the eigenvalue $\lambda = 0$ at $\gamma = 0$. Then the family of such (l_0, m_0, n_0)-modes spans $\mathcal{N}(D_U F(0,0))$. We can directly check the conditions (A1)-(A3) of the simple stationary bifurcation theorem.

Let us take $a = \pi/(2\sqrt{2})$ and $b = \sqrt{3}a$, in oder to see pattern formation clearly after bifurcations. In this case, the eigenvalue $\lambda = 0$ has a two dimensional eigenspace at $\gamma = 0$, namely it is spanned by (l_0, m_0, n_0)-modes with

$$(l_0, m_0, n_0) = (2, 0, 1), \quad (1, 1, 1).$$

The $(2, 0, 1)$-mode is called the "roll-type". The temperature, for instance, has the expression

$$\theta = \theta_{201} \cos(2ax) \sin(\pi z).$$

The $(1, 1, 1)$-mode is called the "rectangle-type". The temperature, for instance, has the expression

$$\theta = \theta_{111} \cos(ax) \cos(\sqrt{3}ay) \sin(\pi z).$$

A special combination of the $(2, 0, 1)$-mode and $(1, 1, 1)$-mode is called the "hexagon-type", which is also an eigenfunction of $\lambda = 0$. The temperature, for instance, has the expression

$$\theta = \theta_{hex}\{2 \cos(ax) \cos(\sqrt{3}ay) + \cos(2ax)\} \sin(\pi z).$$

The isothermal lines of the eigenfunctions of the rectangle and hexagonal-type on the horizontal plane $z = 1/2$ are the follwoing:

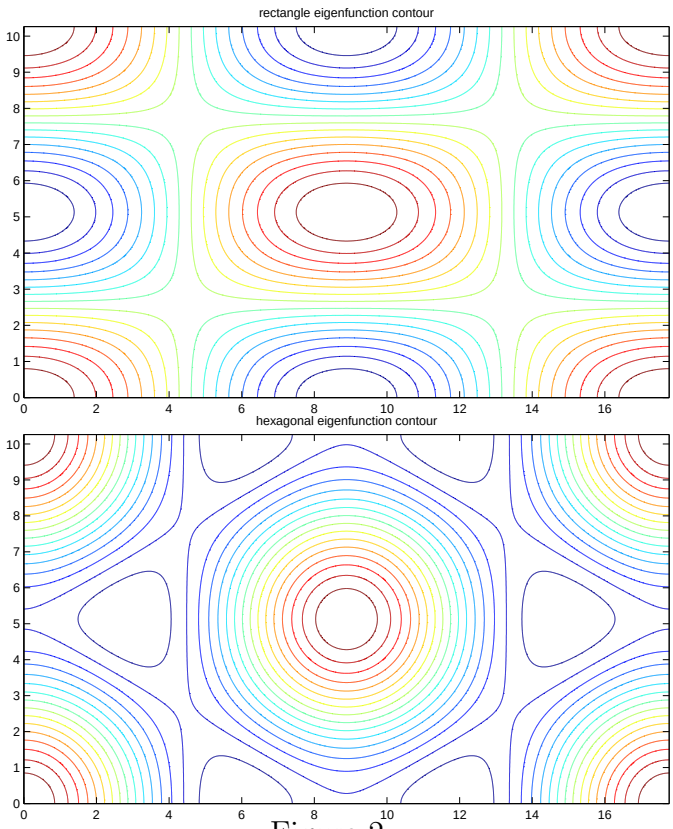

Figure 2.

3.2

The eigenspace has 2-dimension and the simple stationary bifurcation theorem is not directly applicable. We need to restrict the function space $H^2_{a,\sqrt{3}a}$ of the solutions to a subspace, in order to make the eigenspace 1-dimensional there.

First we restrict the function space to the subspace of the roll-type $H^2_{roll} \subset\subset H^2_{a,\sqrt{3}a}$, in which the rectangle-type and hexagon-type are excluded. The temperature, for example, has the expression

$$\theta = \sum_n \sum_{l=even} \theta_{l,0,n} \cos(alx) \sin(n\pi z).$$

The simple stationary bifurcation theorem is applicable in H^2_{roll}, which yields the bifurcated solutions of the roll-type in the direction $\gamma > 0$. The following figures show the contour lines of the stream function and the isothermal lines of the temperature for a bifurcated solution of the roll-type with $\mathcal{P}_r = 10$ and $\gamma = \mathcal{R}_{ac}$:

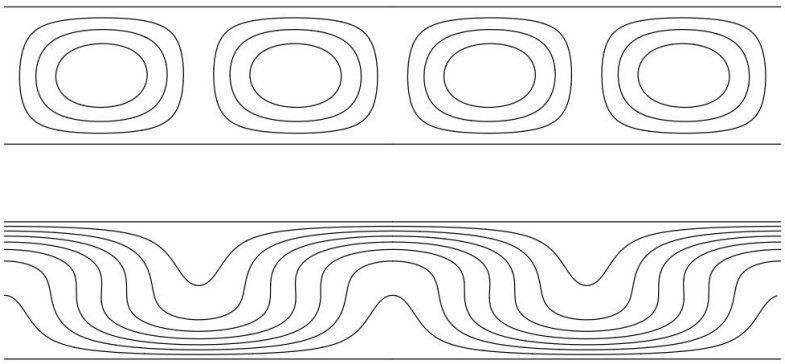

Figure 3.

The bifurcated solutions of the rectangle-type are obtained in the subspace $H^2_{rec} \subset\subset H^2_{a,\sqrt{3}a}$, in which the roll-type and hexagon-type are excluded. The temperature, for example, has the expression

$$\begin{aligned}\theta &= \sum_{n=odd} \sum_{l,m=odd} \theta_{lmn} \cos(alx) \cos(\sqrt{3}amy) \sin(n\pi z) \\ &\quad + \sum_{n=even} \sum_{l,m=even} \theta_{lmn} \cos(alx) \cos(\sqrt{3}amy) \sin(n\pi z).\end{aligned}$$

The simple stationary bifurcation theorem is applicable in H^2_{rec}, which yields the bifurcated solutions of the rectangle-type in the direction $\gamma > 0$. The following figures show the contour lines of the temperature on the middle plane and the absolute value of velocity on the upper surface for a bifurcated solution of the rectacgle-type with $\mathcal{P}_r = 10$ and $\gamma = 0.5\mathcal{R}_{ac}$:

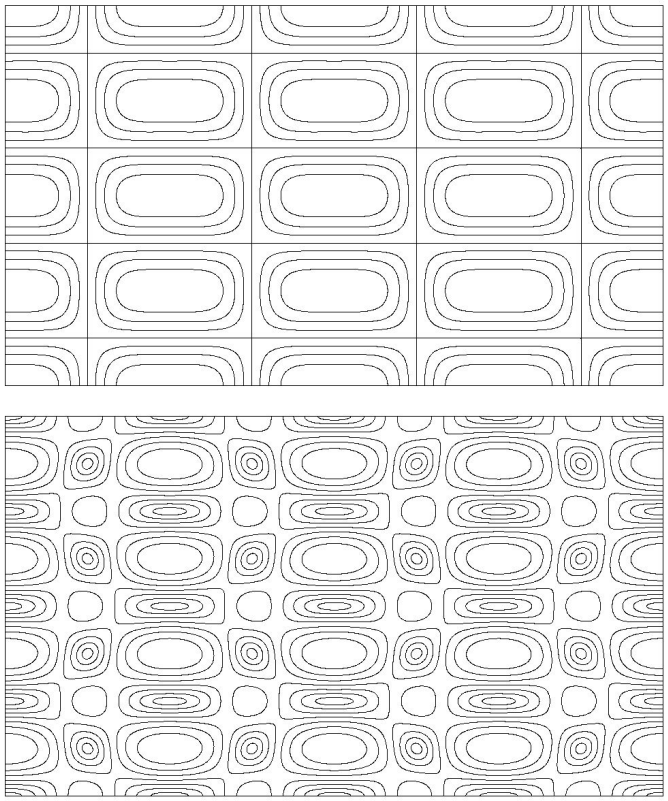

Figure 4.

The bifurcated solutions of hexagonal-type are obtained in the subspace $H^2_{hexa} \subset\subset H^2_{a,\sqrt{3}a}$, in which the roll-type and rectangle-type are excluded. Each element of H^2_{hexa} has the rotation-invariance of $2\pi/3$ and the temperature, for example, has the expression

$$\begin{aligned}\theta &= \sum_{n=odd}\sum_{l+m=even} \theta_{lmn}\{\cos(alx)\cos(\sqrt{3}amy) + \cos(a\frac{l-3m}{2}x)\cos(\sqrt{3}a\frac{l+m}{2}y) \\ &\quad + \cos(a\frac{l+3m}{2}x)\cos(\sqrt{3}a\frac{l-m}{2}y)\}\sin(n\pi z).\end{aligned}$$

The simple stationary bifurcation theorem is applicable in H^2_{hexa}, which yields the bifurcated solutions of the hexagon-type in the direction $\gamma > 0$. The following figures show the contour lines for a bifurcated solution of the hexagon-type with $\mathcal{P}_r = 10$ and $\gamma = \mathcal{R}_{ac}$:

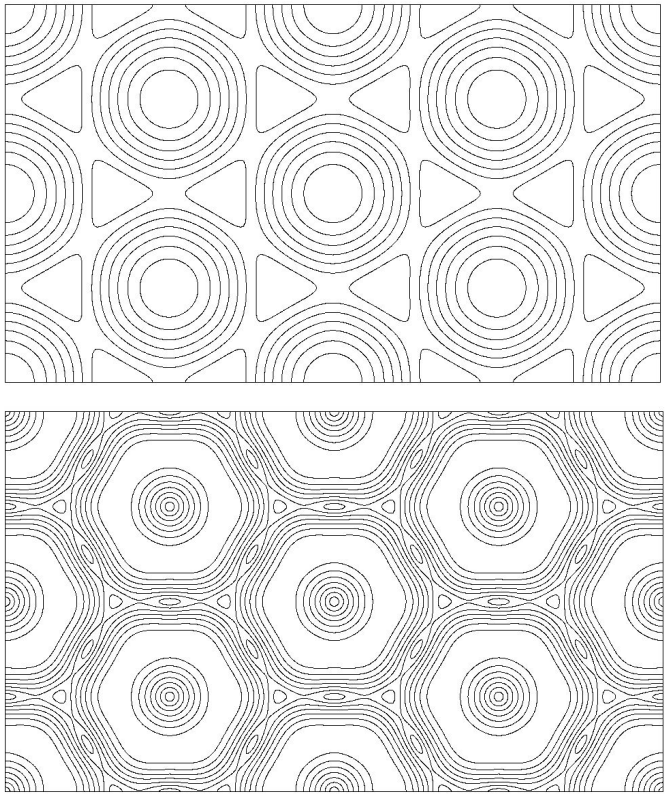

Figure 5.

All of these three types of bifurcated solutions come out of the zero solution at $\gamma = 0$ in the direction $\gamma > 0$ and they belong to their own subspaces. Furthermore, each bifurcated solution is stable in each subspace for the time evolution of the original system. But the stability in the original function space $H^2_{a,\sqrt{3}a}$ is not known, namely it is not clear which type is stable for the time evolution of the original system. The stability of these solutions in the original function space can be determined by the center manifold theory in a neighborhood of the bifurcation point. Now the main problem is to obtain global bifurcation diagrams and to see the global structure of the solution space. At least we want to know how to extend the bifurcation curves, how to analyze the stability of the solution on the extended branches and how to investigate another bifurcation on them such as a secondary bifurcation arising from a bifurcated solution, etc.

4 Computer assisted analysis

4.1

We consider the same system as that of the previous section and trace the stationary solutions on the bifurcation branches for large $\gamma = \mathcal{R}_a - \mathcal{R}_{ac} > 0$. Inserting Fourier series (1.3) into (1.2) and removing time dependency, we have the infinite numbers of second order algebraic equations of the unknowns

$$\{u_{lmn}, v_{lmn}, w_{lmn}, \theta_{lmn}, p_{lmn}\}.$$

We approximate the system of equations by Galerkin's method, namely we approximately solve finite numbers of equations of unknowns

$$\{u_{lmn}, v_{lmn}, w_{lmn}, \theta_{lmn}, p_{lmn} \,|\, l+m+n \le N\}, \tag{4.1}$$

where the approximate solutions tend to an exact one as $N \to \infty$. Let V be the unknowns of (4.1). We write the finite numbers of equations in the form

$$G(V, \gamma) = 0.$$

We solve this equation with a fixed $\mathcal{P}_r$ and γ by Newton's method

$$V_{k+1} = V_k - D_V G(V_k, \gamma)^{-1} G(V_k, \lambda), \;\; k = 0, 1, 2, \cdots,$$

where $D_V G$ is the Fréchet derivative of G and V_0 is appropriately chosen in a neighborhood of an exact solution V. We numerically obtain a solution V with a fixed N by computers. Note that Newton's method works, only if V_0 is close to an exact solutions, regardless of its uniqueness or stability.

The following figures show the cross section $y = \textit{constant}$ of the contour lines of the stream function and isothermal lines for a numerical solution of the roll-type with $\mathcal{P}_r = 10$ and $\gamma = 9\mathcal{R}_{ac}$:

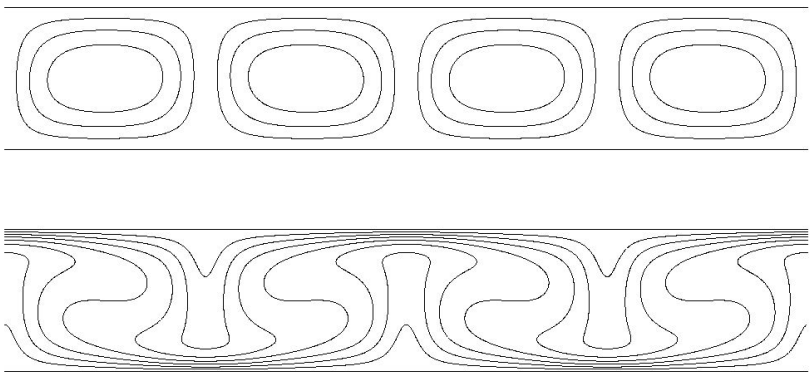

Figure 6.

The stability of the solution follows from the eigenvalues of the evolution system of the linearized system around the obtained solution itself. If all eigenvalues have negative real parts, then it is stable as the time evolution. If one of them has positive real part, then it is not stble. The above solution of the roll-type turns out to be stable.

The following figures show the isothermal lines of the temperature at the middle horizontal plane and the contour lines of the square of the velocity $u^2 + v^2$ on the upper horizontal plane for a numerical solution of the rectangle-type with $\mathcal{P}_r = 10$ and $\gamma = 0.5\mathcal{R}_{ac}$:

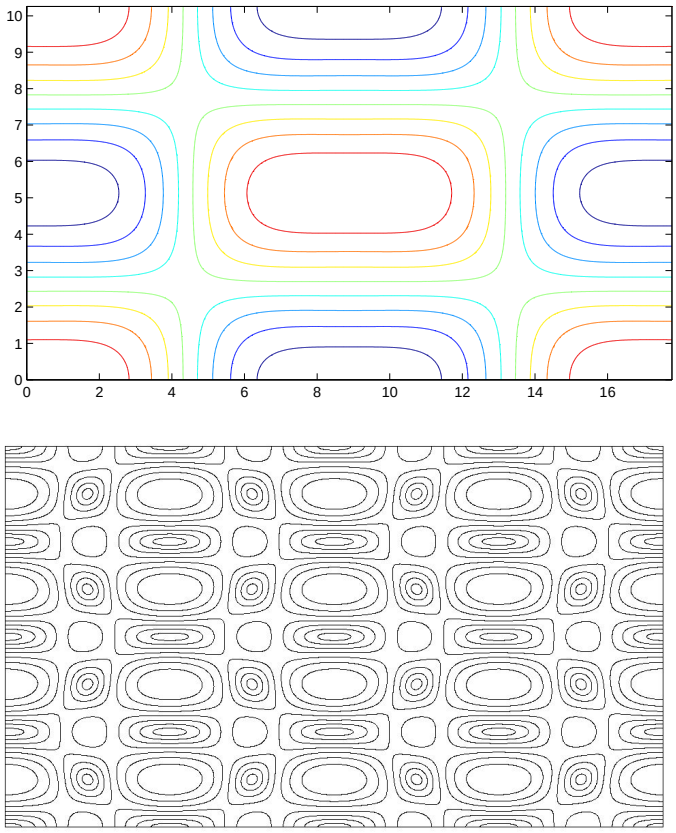

Figure 7.

The solution of rectangle-type is stable for $0 < \gamma < 0.42\mathcal{R}_{ac}$, but it loses the stability at about $\gamma \simeq 0.43\mathcal{R}_{ac}$ and here a secondary bifurcation occurs to a solutions of the mixed type of hexagon and rectangle such as Figure 9. Thus the solution of the rectangle-type of Figure 7 is already unstable.

The following figures show the contour lines and isothermal lines for a numerical solution of the hexagon-type with $\mathcal{P}_r = 10$ and $\gamma = \mathcal{R}_{ac}$:

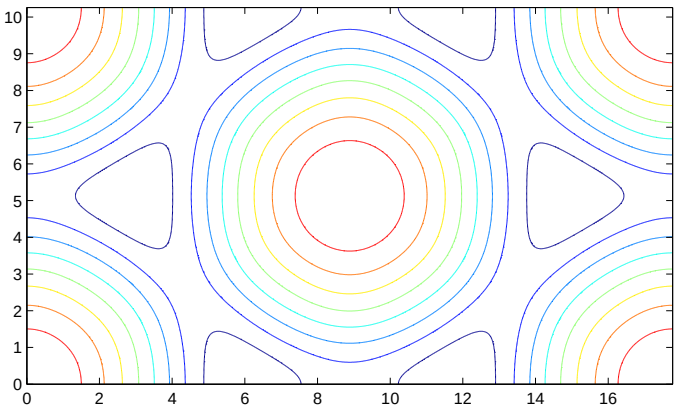

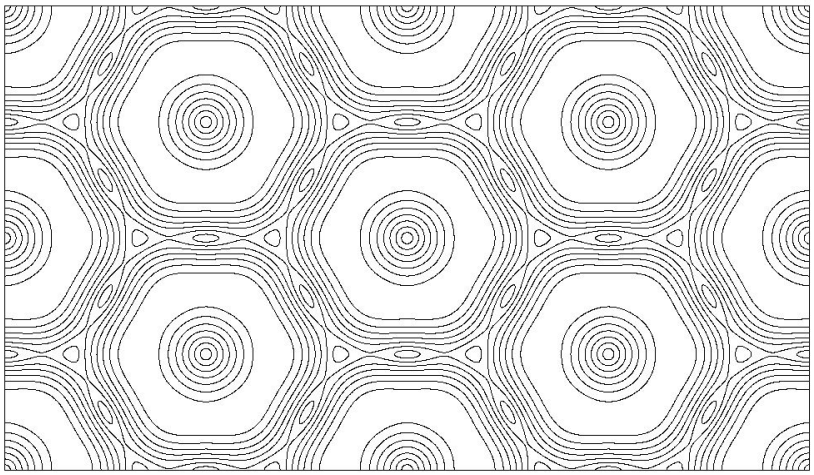

Figure 8.

The solutions of the hexagon-type are unstable just after the bifurcation for $0 < \gamma < 0.83\mathcal{R}_{ac}$. However after the bifurcation branch of the hexagon-type and that of the mixed type intersects at about $\gamma \simeq 0.84\mathcal{R}_{ac}$, it becomes stable for $0.85\mathcal{R}_{ac} < \gamma$. The hexagon of Figure 8 is already stable.

The following figures show the contour lines and isothermal lines for a numerical solution of the mixed type with $\mathcal{P}_r = 10$ and $\gamma = 0.5\mathcal{R}_{ac}$:

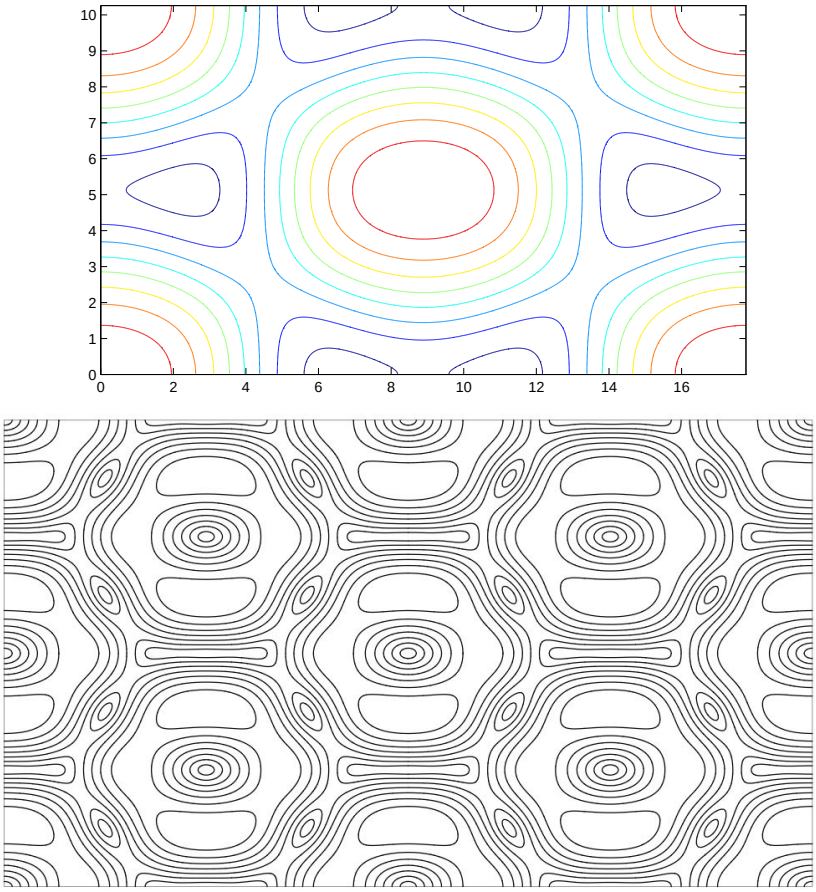

Figure 9.

The solution in Figure 9 is just after the secondary bifurcation to the mixed type from the rectangle-type. It is stable for $0.44\mathcal{R}_{ac} < \gamma < 0.83\mathcal{R}_{ac}$ and the shape of the mixed type tends to that of the hexagon-type as γ increases. After the intersection with the hexagonal bifurcation branch, it becomes unstable and the shape becomes elongated in y-direction.

The following figure shows a rough diagram of the bifurcations: The horizontal axis means the trivial solution (the heat conduction state). The upper line serves the bifurcation curve of the roll-type and the lowest line serves that of the rectangle-type, which appear at $\gamma = 0$. They are orthogonal to each other. The line between them serves that of the hexagon-type. The secondary bifurcation branch from the branch of the rectange-type serves that of the mixed type. It intersects with that of the hexagon-type. The hexagon-type becomes stable after this intersection. The roll-type is stable for all $0 < \gamma \leq 2\mathcal{R}_{ac}$. The justification of this bifurcation diagram is a problem in the future, namely the proof of the bifurcation curves, the secondary bifurcations, the intersections of those curves, those stability and so on. We will treat the roll-type solution later as a computer assisted proof.

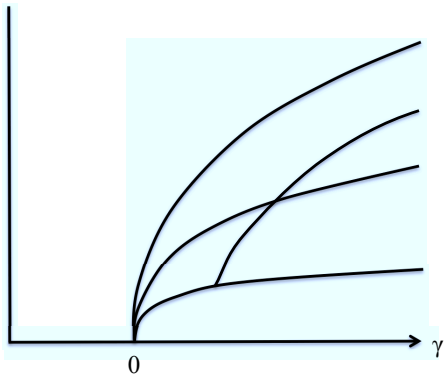

Figure 10.

4.2

Now we deal with (1.2) under the stress free upper boundary and fixed bottom boundary (the case 2 in 1.2). We will consider the bifurcation problems under the assumption of periodicity and also usual even- or odd-ness of functions for all unkowns in the horizontal direction:

$$
\begin{aligned}
&u(x,y,z) = -u(-x,y,z) = u(x,-y,z),\\
&v(x,y,z) = v(-x,y,z) = -v(x,-y,z),\\
&w(x,y,z) = w(-x,y,z) = w(x,-y,z),\\
&\theta(x,y,z) = \theta(-x,y,z) = \theta(x,-y,z),\\
&p(x,y,z) = p(-x,y,z) = p(x,-y,z).
\end{aligned}
$$

Then the first component of the velocity and the temperature, for instance, have the expansions

$$\begin{aligned} u(x,y,z) &= \sum_{l,m} u_{lm}(z)\sin(alx)\cos(bmy), \\ \theta(x,y,z) &= \sum_{l,m} \theta_{lm}(z)\cos(alx)\cos(bmy). \end{aligned}$$

The other unknown functions have similar expansions.

The system for the eigenvalue problem can be obtained as the following system of ordinary differential equations with respect to z for each (l,m)-mode:

$$\begin{aligned} \lambda u_{lm} - \mathcal{P}_r alp_{lm} &= \mathcal{P}_r\{\frac{d^2}{dz^2} - (a^2l^2+b^2m^2)\}u_{lm}, \\ \lambda v_{lm} - \mathcal{P}_r bmp_{lm} &= \mathcal{P}_r\{\frac{d^2}{dz^2} - (a^2l^2+b^2m^2)\}v_{lm}, \\ \lambda w_{lm} - \mathcal{P}_r \frac{d}{dz}p_{lm} &= \mathcal{P}_r\{\frac{d^2}{dz^2} - (a^2l^2+b^2m^2)\}w_{lm} + \mathcal{P}_r\mathcal{R}_a\theta_{lm}, \\ \lambda\theta_{lm} &= \{\frac{d^2}{dz^2} - (a^2l^2+b^2m^2)\}\theta_{lm} + w_{lm}, \\ alu_{al} + bmv_{lm} + \frac{d}{dz}w_{lm} &= 0 \end{aligned}$$

with the boundary conditions

$$\begin{aligned} \frac{du}{dz} = \frac{dv}{dz} = w = \theta = 0 \qquad & \text{on } z = 1, \\ u = v = w = \theta = 0 \qquad & \text{on } z = 0. \end{aligned}$$

We solve this system by computers. In order to obtain the critical Rayleigh number numerically, we may use the Chebyshev polynomial expansion in $0 \le z \le 1$ for our system of ordinary differential equations. Then, by the numerical computations, we obtain the following values, at which the largest eigenvalue becomes zero:

$$\begin{aligned} a/\pi = 0.42685\cdots &> \frac{1}{2\sqrt{2}}, \\ \mathcal{R}_{ac} = 1100.6\cdots &> 6.75\times\pi^4, \end{aligned}$$

where the values of the right-hand side of the inequalities correspond to the case 1 in 1.2, namely the stress free boundary conditions on both boundaries. The following figures show the eigenfunctions θ and w of the eigenvalue $\lambda = 0$ for the critical Raleigh number $\mathcal{R}_a = \mathcal{R}_{ac} = 1100.6\cdots$:

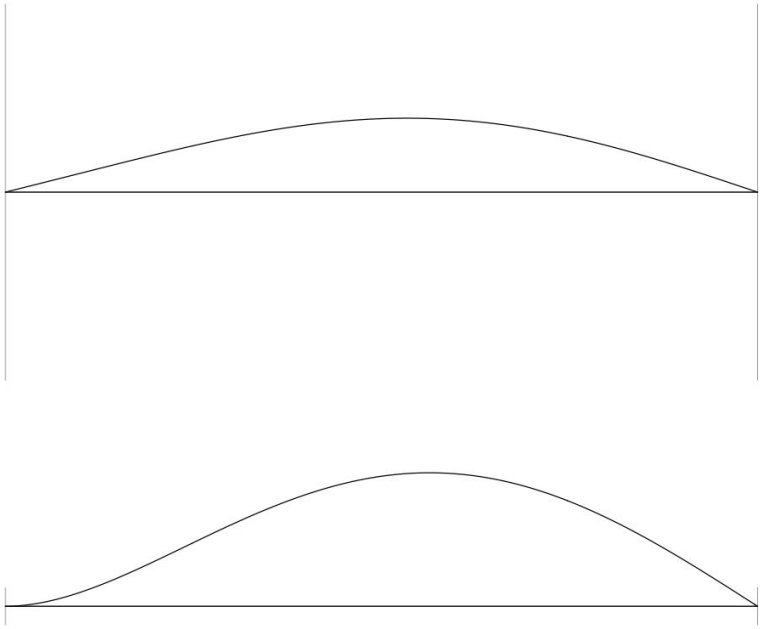

Figure 11.

The largest eigenvalue crossing the origin determines the critical Rayleigh number $\mathcal{R}_{ac}$, which yields a stationary bifurcation. If $\mathcal{R}_a < \mathcal{R}_{ac}$, then the heat conduction state is linearly stable. If $\mathcal{R}_a > \mathcal{R}_{ac}$, then the heat conduction state is linearly unstable. Joseph proved by the energy method and variational formulation that if $\mathcal{R}_a < \mathcal{R}_{ac}$, then the heat conduction state is globally nonlinearly stable.

Now we study the bifurcation of stationary solutions. In order to see pattern formations after the bifurcation clearly, let us take $a = 0.42685\cdots$ and $b = \sqrt{3}a$. The eigenvalue $\lambda = 0$ has a 2-dimensional eigenspace at $\mathcal{R}_a = 1100.6\cdots$.

The mode $(l, m) = (2, 0)$ corresponds to the roll-type and the eigenfunction of the temperature is of the form

$$\theta = \theta_{2,0}(z)\cos(2ax).$$

The mode $(l, m) = (1, 1)$ corresponds to the rectangle-type and the eigenfunction of the temperature is of the form

$$\theta = \theta_{1,1}(z)\cos(ax)\cos(\sqrt{3}ay).$$

A special combination of the roll-type and rectangle-type corresponds to the hexagon-type and the eigenfunction of the temperature is of the form

$$\theta = \theta_{hexa}(z)\{2\cos(ax)\cos(\sqrt{3}ay) + \cos(2ax)\}.$$

The isothermal lines of the eigenfunctions of the rectangle and hexagonal-type are the follwoing:

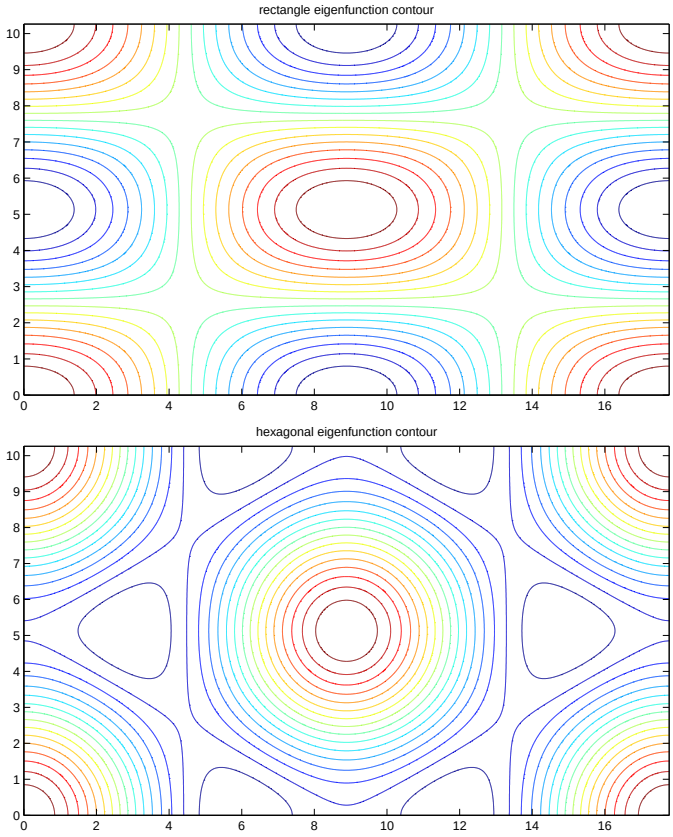

Figure 12.

The eigenspace has 2-dimension and the simple stationary bifurcation theorem is not directly applicable. We need to restrict the function space $H^2_{a,\sqrt{3}a}$ of the solutions to a subspace, in order to make the eigenspace 1-dimensional there.

We restrict the space to the subspace of the roll-type $H^2_{roll} \subset\subset H^2_{a,\sqrt{3}a}$. The temperature, for example, has the expression

$$\theta = \sum_n \sum_{l=even} \theta_{l,0,n} \cos(alx) T_n(2z-1),$$

where T_n are the Chebyshev polynomials. We have the bifurcated solutions of the roll-type in the direction of $\mathcal{R}_a > \mathcal{R}_{ac}$. The following figure shows the isothermal lines of the temperature at the cross section $y = constant$ for a bifurcated solution of the roll-type with $\mathcal{P}_r = 10$ and $\mathcal{R}_a = 1.2\mathcal{R}_{ac}$.

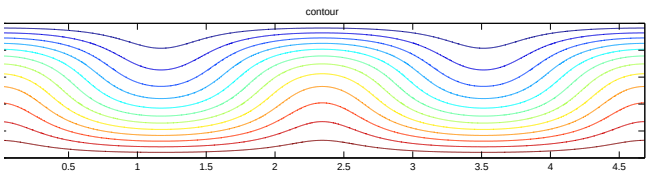

Figure 13.

Similarly we restrict the space to the subspace of the rectangle-type $H^2_{rec} \subset\subset H^2_{a,\sqrt{3}a}$ and the hexagon-type $H^2_{hexa} \subset\subset H^2_{a,\sqrt{3}a}$, in which the simple stationary bifurcation theorem is applicable. The stability of these bifurcated solutions in the original function space

$H^2_{a,\sqrt{3}a}$ is not known. The stability of these solutions in the original function space can be determined by the center manifold theory in a neighborhood of the bifurcation point. The main problem is to obtain global bifurcation diagrams and to see the global structure of the solution space. At least we want to know how to extend the bifurcation curves, how to analyze the stability of the solution on the extended branches and how to investigate another bifurcations on them, i.e., the secondary bifurcations and so on.

In order to extend the bifurcation curves of the stationary solutions, we need to make numerical computations for the stationary problem of (1.2). We may use of the Chebyshev polynomial expansion for the solutions in z, where the unknown $u(x, y, z)$, for example, is expanded as

$$u(x, y, z) = \sum_{l,m,n} u_{lmn} \sin(alx) \cos(bmy) T_n(2z - 1).$$

Then $\{u_{lmn}, v_{lmn}, w_{lmn}, \theta_{lmn}, p_{lmn}\}$ are unknowns and satisfy the second order algebraic equations of infinite numbers. We approximate the system of equations by Galerkin's method, namely we approximately solve finite numbers of equations of unknowns

$$\{u_{lmn}, v_{lmn}, w_{lmn}, \theta_{lmn}, p_{lmn} \,|\, l + m < M,\ n \le N\}, \tag{4.2}$$

where the approximate solutions tend to an exact one as $M, N \to \infty$. Let V be the unknowns of (4.2). We write the finite numbers of equations in the form

$$G(V; \mathcal{R}_a, \mathcal{P}_r) = 0.$$

We solve this equation with a fixed $\mathcal{R}_a$ and $\mathcal{P}_r$ by Newton's method

$$V_{k+1} = V_k - D_V G(V_k, \gamma)^{-1} G(V_k, \lambda), \quad k = 0, 1, 2, \cdots,$$

where $D_V G$ is the Fréchet derivative of G and V_0 is appropriately chosen in a neighborhood of an exact solution V. We numerically obtain a solution V with a fixed M and N by computers. Note that Newton's method works, only if V_0 is close to an exact solutions, regardless of its uniqueness or stability. We make numerical computations by Newton method for the solution of roll-, hexagon- and mixed-type

The following figures show the cross section $y = constant$ of two bifurcated solutions of the roll-type with $\mathcal{R}_a = 2\mathcal{R}_{ac}$ and $\mathcal{R}_a = 10\mathcal{R}_{ac}$:

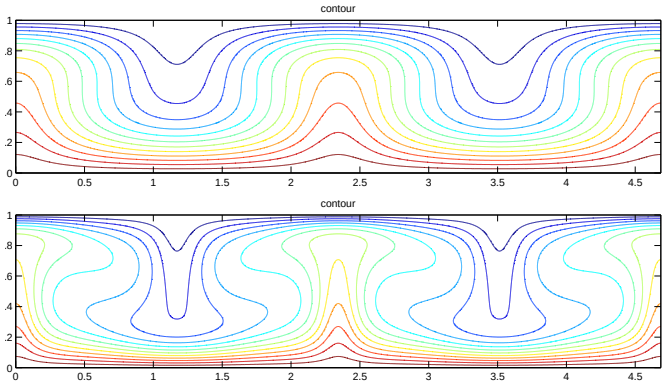

Figure 14.

We obtain the bifurcated solutions of the roll-type with $\mathcal{R}_a$ up to $\mathcal{R}_a \leq 50\mathcal{R}_{ac}$. The following figure shows the bifurcation curve of the roll-type for $1 \leq r := \mathcal{R}_a/\mathcal{R}_{ac} \leq 50$, where the horizontal axis stands for the normalized Rayleigh number $r = \mathcal{R}_a/\mathcal{R}_{ac}$ and the vertical axis stands for the coefficient $u_{2,0,1}$ of the expansion of the solution:

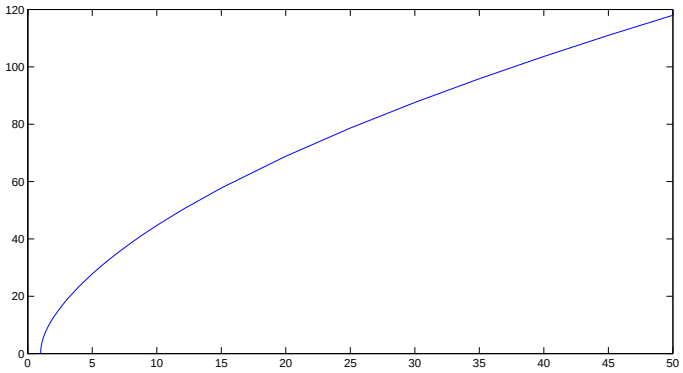

Figure 15.

The following figures shows the isothermal lines of two bifurcated solutions of the hexagon-type with $\mathcal{R}_a = 1.5\mathcal{R}_{ac}$: The fluid is sinking around the center of the hexagon in the first one and is going up in the second one.

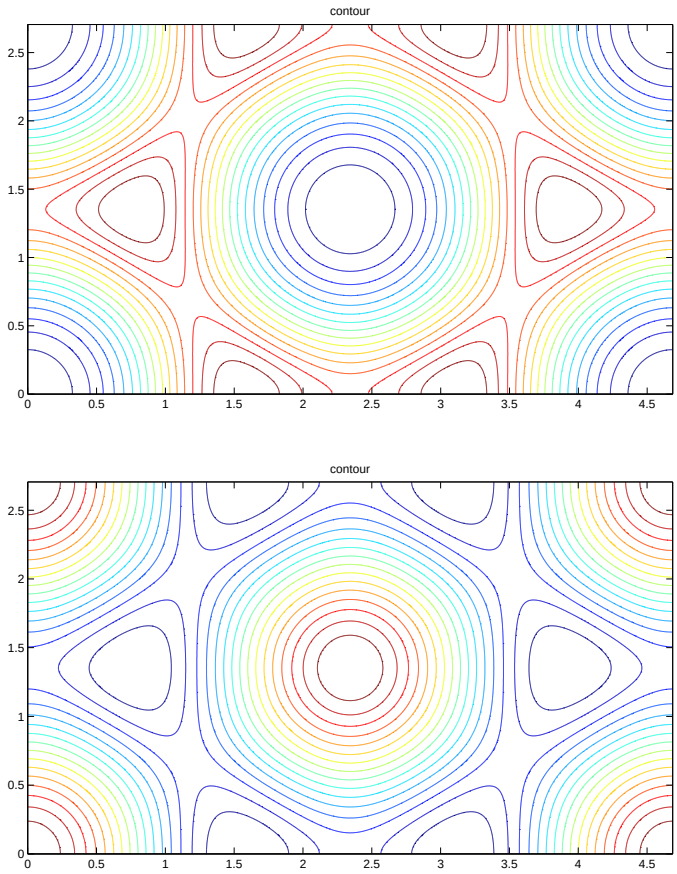

Figure 16.

We also have solutions of mixed type of rectangle and hexagon. The following figures shows the isothermal lines of two bifurcated solutions of mixed type with $\mathcal{R}_a = 1.1\mathcal{R}_{ac}$ and $\mathcal{R}_a = 1.6\mathcal{R}_{ac}$:

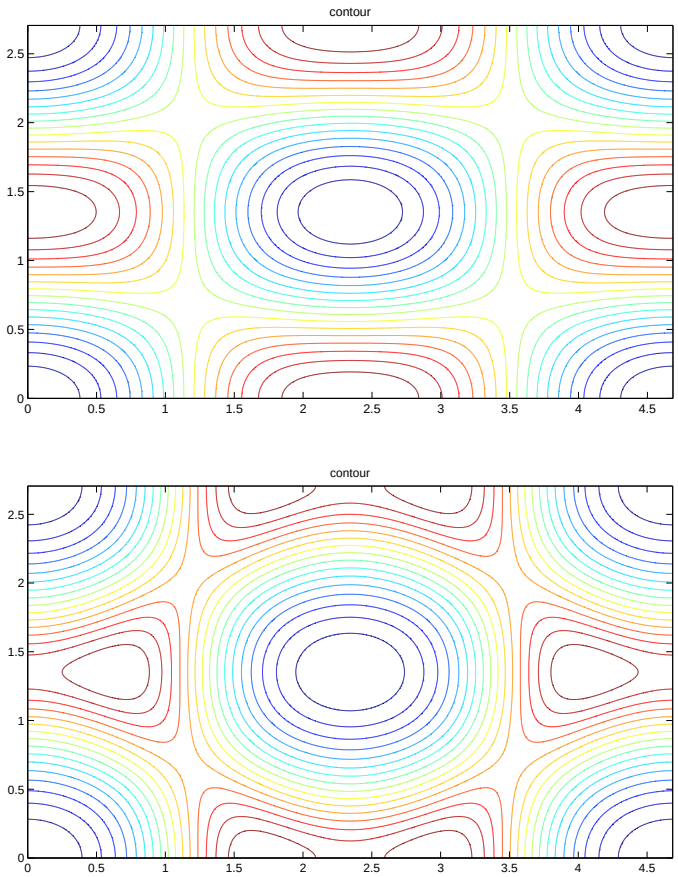

Figure 17.

The bifurcation curve of the mixed type begins from the first bifurcation point $\mathcal{R}_a = \mathcal{R}_{ac}$, at which it corresponds to the eigenfunction of the rectangle-type. The bifurcation curves of the hexagon-type and mixed type, of which the fluid is sinking around the center, are given by the following: The horizontal axis stands for the normalized Rayleigh number $r = \mathcal{R}_a/\mathcal{R}_{ac}$ and the vertical axis stands for the coefficient $u_{2,0,1}$ of the expansion of the solution.

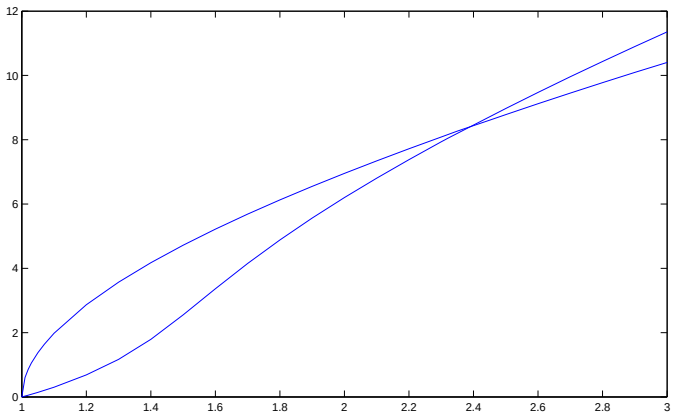

Figure 18.

The following figures show the isothermal lines of a solution of the mixed type and hexagon-type with $\mathcal{R}_a = 3\mathcal{R}_{ac}$ after the intersection of the bifurcation curves:

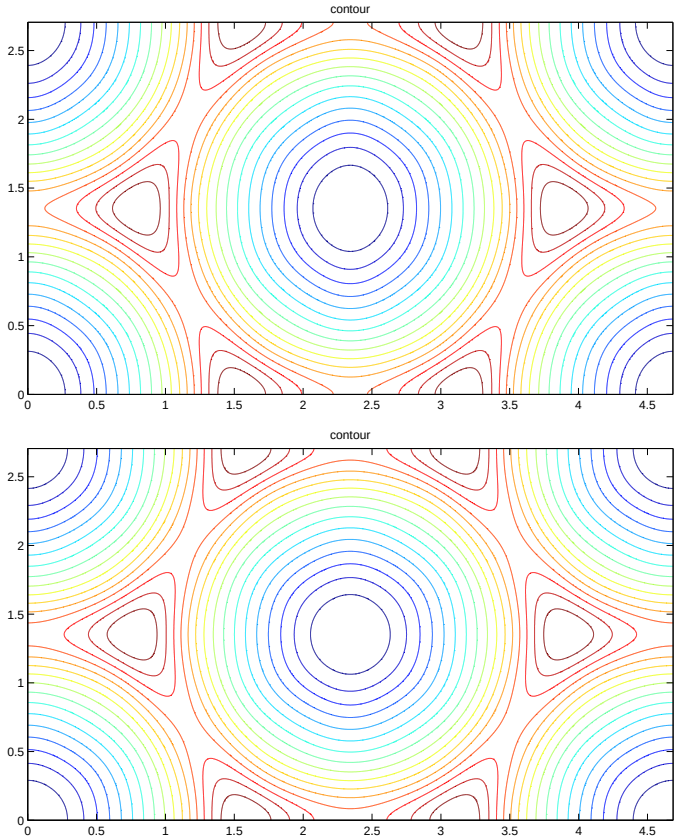

Figure 19.

There is another bifurcation branch of the mixed type. The following figures shows the isothermal lines of a solution on this branch with $\mathcal{R}_a = 1.63\mathcal{R}_{ac}$ and $\mathcal{R}_a = 1.8\mathcal{R}_{ac}$:

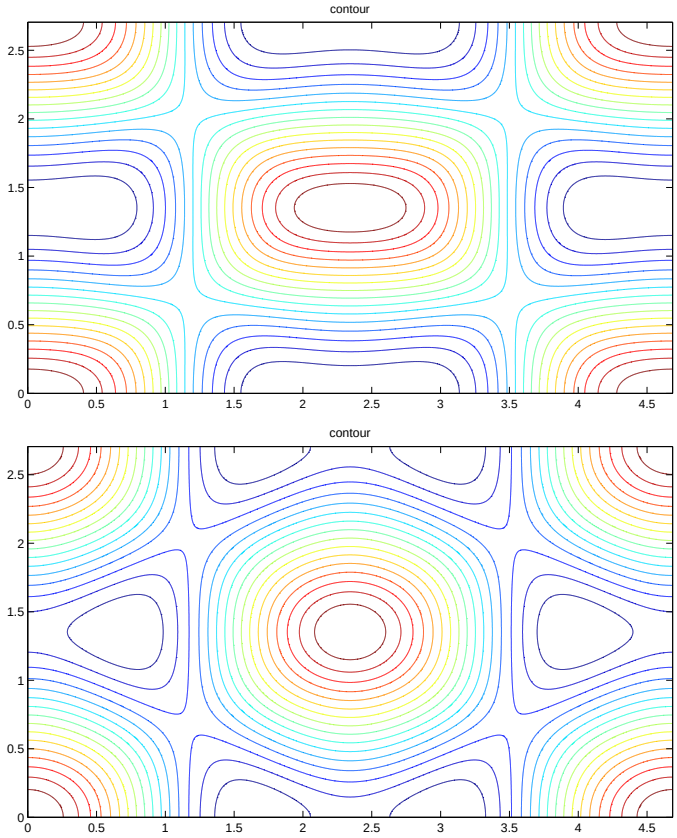

Figure 20.

The bifurcation curve of this mixed type approaches to that of the hexagon-type, of which the fluid is going up around the center. In fact we have the bifurcation curves which cross near $\mathcal{R}_a = 2.02\mathcal{R}_{ac}$ as follows:

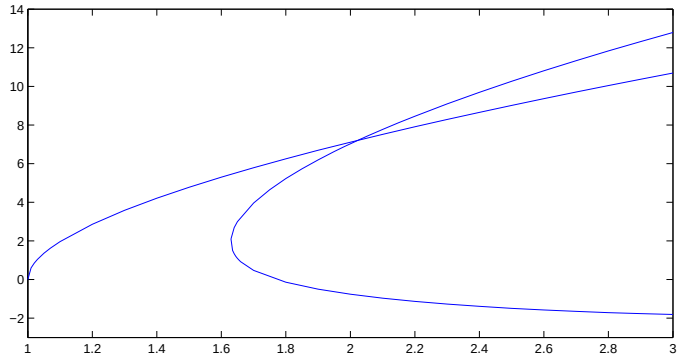

Figure 21.

The following figures show the isothermal lines of a solution of this mixed type and a solution of the hexagon-type with $\mathcal{R}_a = 3\mathcal{R}_{ac}$ (this is after the intersection of the bifurcation curves):

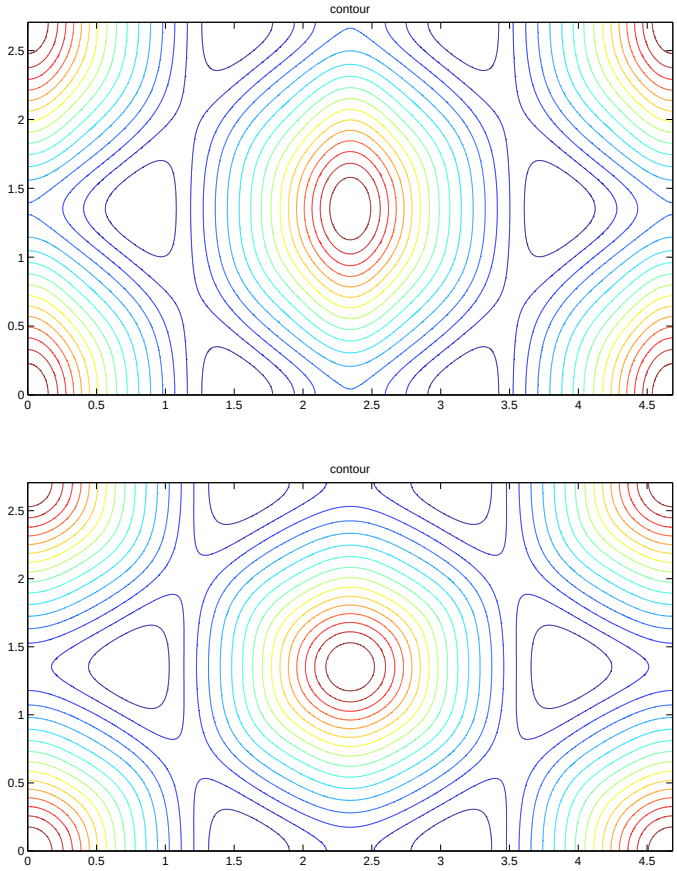

Figure 22.

5 Computer assisted proofs

5.1

We consider a constructive approximation to the solutions of the system of semilinear partial differential equations with large Rayleigh numbers. There is a theorem which guarantees the existence of Galerkin approximate solutions as precise as you want if the solution is isolated. The idea has been used by Urabe in 1960's for the system of ordinary differential equations. Also we have a theorem which guarantees an existence of a genuine solution in a small neighborhood of a "good" approximate solution. It is a simplified Newton's method for the Schauder's fixed point theorem in the following setting:

Let $U \subset V \subset W$ be Banach spaces, in which the embedding $U \subset V$ is compact. Consider the semilinear equation

$$\mathcal{F}(u) := Au + B(u,u) = 0,$$

where $A : U \to W$ is linear operator and $B : V \times V \to W$ is bilinear operator such that

$$\| B(u,v) \|_W \leq K \| u \|_V \| v \|_V, \quad \| B(u,v) \|_V \leq K \| u \|_U \| v \|_U .$$

The N-dimensional projection $P_N : W \to W_N$ commutes with A and satisfies the following: For any $N > 0$ and all $v \in V,\ u \in U$

$$\| v_N - v \|_W \leq \frac{1}{N} \| v \|_V \quad (v_N := P_N v),$$
$$\| u_N - u \|_V \leq \frac{1}{N} \| u \|_U \quad (u_N := P_N u,).$$

Theorem. *Let $\bar{u} \in U_N$ be a good approximate solution in the sense that*

$$A\bar{u} + P_N B(\bar{u}, \bar{u}) = R_N, \quad \| R_N \|_W < \varepsilon \ll 1,$$

and that for the linearized equation around this approximate solution given by

$$L(\bar{u})v := Av + B(\bar{u}, v) + B(v, \bar{u}) = f \quad (f \in W)$$

there exists $\tilde{K} < \infty$ independent of f such that

$$\| L^{-1}(\bar{u}) f \|_U \leq \tilde{K} \| f \|_W .$$

If $\tilde{\varepsilon} := \| B(\bar{u}, \bar{u}) - P_N B(\bar{u}, \bar{u}) \|_W \ll 1$ and we can find α such that $\tilde{K}(\varepsilon + \tilde{\varepsilon} + K\alpha^2) < \alpha$, then there exists a genuine solution $u \in U \cap \mathcal{W}$ of $\mathcal{F}(u) = 0$, where $\mathcal{W} := \{u \in V \mid \| u - \bar{u} \|_V < \alpha\}$.

Proof. We look for a solution u to $Au + B(u, u) = 0$ of the form

$$u = \bar{u} + v.$$

Then v should satisfy the equation

$$v = -L(\bar{u})^{-1}\{(A\bar{u} + P_N B(\bar{u}, \bar{u})) + (B(\bar{u}, \bar{u}) - P_N B(\bar{u}, \bar{u})) + B(v, v)\}. \tag{5.1}$$

Let us define a map $\mathcal{G}$ from $\tilde{\mathcal{W}} := \{v \in V \mid \| v \|_V < \alpha\}$ to W as

$$\mathcal{G}(v) := -L(\bar{u})^{-1}\{(A\bar{u} + P_N B(\bar{u}, \bar{u})) + (B(\bar{u}, \bar{u}) - P_N B(\bar{u}\bar{u})) + B(v, v)\}.$$

It follows from the assumption that for any $v \in \tilde{\mathcal{W}}$

$$\| \mathcal{G}(v) \|_V \leq \tilde{K}(\varepsilon + \tilde{\varepsilon} + K\alpha^2) < \alpha$$

and $\mathcal{G}(v) \in \tilde{\mathcal{W}}$. Therefore we have a fixed point of $\mathcal{G}$ by Shauder's fixed point theorem, which yields a solution of (5.1) in $\tilde{\mathcal{W}}$. □

5.2

We consider again the stationary solutions of the roll-type to (1.2) with the stress free boundary conditions (the case 1 in 1.2). In oder to obtain such solutions for large Rayleigh numbers, we have to exploit numerical computations. We want to justify a numerical solution in the sense that there does exist a genuine solution close to the numerical solution and the error between them can be controlled.

We can use the stream function ψ instead of the velocity, since the roll-type is 2-dimensional in space. The new equation is of the form

$$\begin{aligned}\frac{\partial}{\partial t}\Delta\psi &= \mathcal{P}_r\mathcal{R}_a\Delta^2\psi + \mathcal{R}_a\frac{\partial\theta}{\partial x} + \frac{\partial\psi}{\partial z}\frac{\partial}{\partial x}\Delta\psi - \frac{\partial\psi}{\partial x}\frac{\partial}{\partial z}\Delta\psi,\\ \frac{\partial\theta}{\partial t} &= \Delta\theta + \frac{\partial\psi}{\partial x} + \frac{\partial\psi}{\partial z}\frac{\partial\theta}{\partial x} - \frac{\partial\psi}{\partial x}\frac{\partial\theta}{\partial z}\end{aligned}$$

with the stress free boundary conditions for $z = 0, 1$. The function space is $H^4 \otimes H^2$ with the periodicity. The stationary solutions have the Fourier expansion

$$\psi(x,z) = \sum_{l,n}\psi_{ln}\sin(alx)\sin(n\pi z), \quad \theta(x,z) = \sum_{l,n}\theta_{ln}\cos(alx)\sin(n\pi z).$$

First we numerically investigate the bifurcation curve of the roll-type for large Rayleigh numbers. The following figure shows the bifurcation curve of $\psi_{2,1}$ of the roll-type for $\mathcal{R}_c \le \mathcal{R}_a \le 50\mathcal{R}_{ac}$:

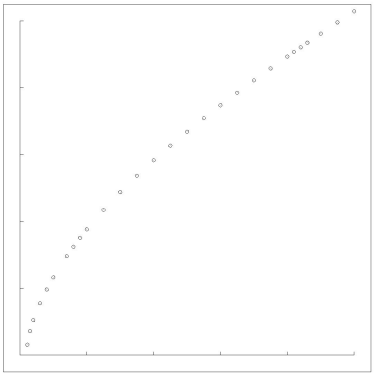

Figure 23.

These solutions of the roll-typeare stable for $\mathcal{R}_a < 41\mathcal{R}_c$, but the eigenvalue of the linearized system crosses the imaginary axis at about $\mathcal{R}_a \simeq 42\mathcal{R}_{ac}$. Then it becomes unstable and there occurs the Hopf bifurcation. The shape of solutions of the roll-type are almost same before and after the stability change. The following figures show solutions of the roll-type with $\mathcal{R}_a = 40\mathcal{R}_{ac}$ in the first couple of figures and $\mathcal{R}_a = 43\mathcal{R}_{ac}$ in the second one:

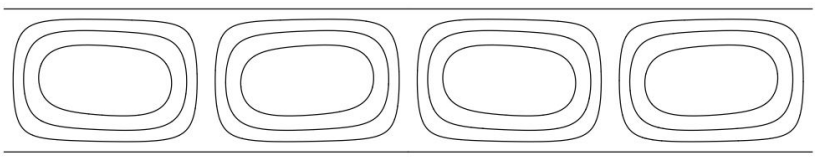

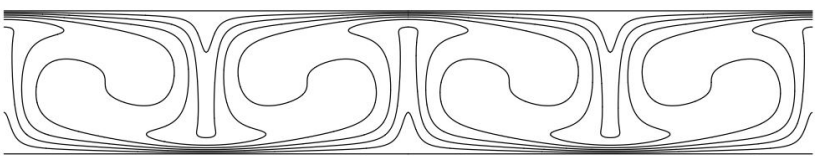

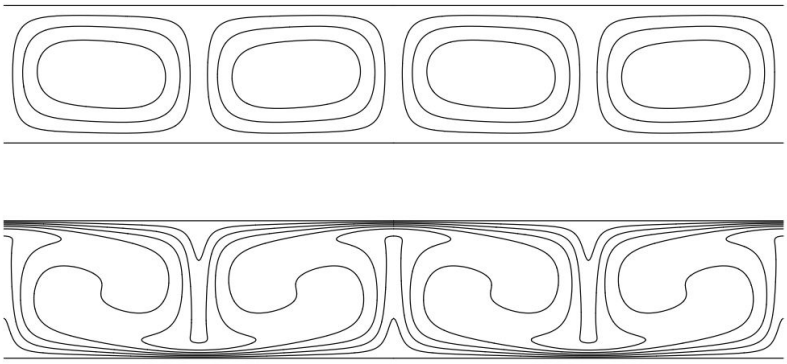

Figure 24.

The time periodic solution after the Hopf bifurcation can be obtained by the numerial computations of time evolution of the system with time discretization as follows:

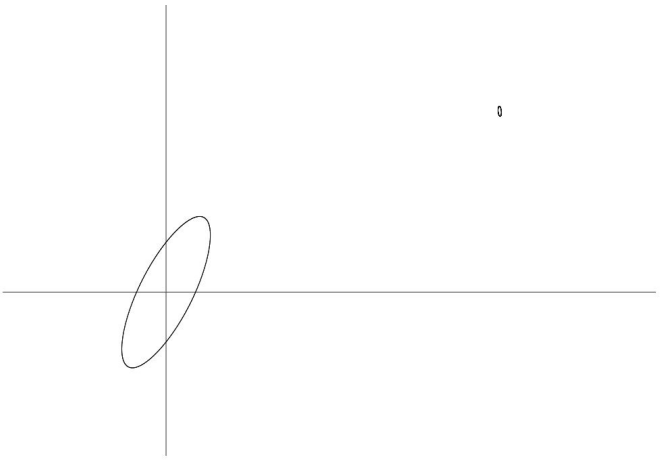

Figure 25.

This suggests that the periodic solution is stable, contrary to the bifurcation of periodic solutions of Lorenz model (1963).

In order to prove the existence of stationary solutions of the roll-type far from the first bifurcation point $\mathcal{R}_a = \mathcal{R}_{ac}$ through numerical computations, we transform our problem to a fixed point formulation in the function space $H^3 \otimes H^1$ with the inverse operators of Δ^2 and Δ with the stress free boundary conditions as follows:

$$\begin{aligned} \psi &= -\frac{1}{\mathcal{P}_r \mathcal{R}_a}\{\Delta^{-2}(\mathcal{R}_a \frac{\partial \theta}{\partial x} + \frac{\partial \psi}{\partial z}\frac{\partial}{\partial x}\Delta\psi - \frac{\partial \psi}{\partial x}\frac{\partial}{\partial z}\Delta\psi)\}, \\ \theta &= -\Delta^{-1}(\frac{\partial \psi}{\partial x} + \frac{\partial \psi}{\partial z}\frac{\partial \theta}{\partial x} - \frac{\partial \psi}{\partial x}\frac{\partial \theta}{\partial z}). \end{aligned}$$

The nonlinear operators in the right hand side are compact in the space $H^3 \otimes H^1$. We write the above equation with

$$\mathcal{F}_0(\psi, \theta) = (\psi, \theta).$$

We look for a solution as a fixed point of $\mathcal{F}_0$. The solution is sought in the form

$$(\psi, \theta) = (\bar{\psi}_N, \bar{\theta}_N) + (w^{(1)}, w^{(2)}),$$

where $(\bar{\psi}_N, \bar{\theta}_N)$ is a numerically computed "good" solution. Then the equation of $w = (w^{(1)}, w^{(2)})$ can be written as

$$\mathcal{G}(w) = w.$$

If we find a bounded closed convex set $\tilde{\mathcal{W}}$ such that $\mathcal{G}(\tilde{\mathcal{W}}) \subset \tilde{\mathcal{W}}$ for fixed $\mathcal{R}_a$ and $\mathcal{P}_r$, then there exists a fixed point by Schauder's fixed point theorem, which proves the existence of a genuine stationary solution of the roll-type. The set $\tilde{\mathcal{W}}$ is constructed as a small neighborhood of the origin and the inclusion $\mathcal{G}(\tilde{\mathcal{W}}) \subset \tilde{\mathcal{W}}$ is verified by numerical computations as a computer assisted proof with interval arithmetics. In fact we decompose the set by the orthogonal projection P_N

$$\tilde{\mathcal{W}} = \tilde{\mathcal{W}}_N \oplus \tilde{\mathcal{W}}_N^{\perp},$$

where $\tilde{\mathcal{W}}_N := P_N \tilde{\mathcal{W}}$ is a finite dimensional small neighborhood of the origin and $\tilde{\mathcal{W}}_N^{\perp}$ is a small neighborhood of zero in the orthogonal subspace with infinite dimension. The finite dimensional part is estimated by a simplified Newton's method and the infinite dimensional part is estimated by the norm. Both estimates need the interval arithmetic by computers for error estimates. At the present stage, the case with Rayleigh numbers $\mathcal{R}_c < \mathcal{R}_a \leq 10\mathcal{R}_c$ can be verified by our computer assisted proofs in the 2-dimensional problems (Watanabe-Yamamoto-Nakao-Nishida, 2004). The 3-dimensional problems, namely the solutions of the hexagon-type and mixed type, can be verified by our computer assisted proofs for small Rayleigh numbers $\mathcal{R}_c < \mathcal{R}_a < 1.2\mathcal{R}_c$, because of the limitation of computer power (Kim-Nakao-Watanabe-Nishida, 2008).

References

[1] Bénard, H., Les tourbillons cellulaires dans une nappe liquide, Revue Gén. Sci. Pure Appl. 11 (1900) pp.1261-1271, pp.1309-1328.

[2] Busse, F. H., Nonlinear properties of thermal convection, Rep. Prog. Phys. 41 (1978) 1929-1967.

[3] Boussinesq, J., Théorie analytique de la chaleur, Vol.2. Paris, Gauthier-Villars (1903).

[4] Crandall, M. G. and Rabinowitz, P. H., Bifurcation, perturbation of simple eigenvalues, and linearized stability, Arch. Rat. Mech. Anal. 52 (1973) 161-180.

[5] Crandall, M. G. and Rabinowitz, P. H., The Hopf bifurcation theorem in infinite dimensions, Arch. Rat. Mech. Anal. 67 (1977) 53-72.

[6] Fujimura, Kaoru and Yamada, Syouko, The 1:2 spatial resonance on a hexagonal lattice in two-layered Rayleigh-Bénard problems, Proc. R. Soc. A. 464 (2007) 133-153.

[7] Golubitsky, M., Swift, J. W. and Knobloch, E., Symmetries and pattern selection in Rayleigh-Bénard convection, Physica D. 10 (1984) 249-276.

[8] Henry, D., Geometric Theory of Semilinear Parabolic Equations, Springer-Verlag 1981.

[9] Iohara, T., Nishida, T., Teramoto, Y. and Yoshihara, H., Bénard-Marangoni convection with a deformable surface, Kokyuroku, RIMS, Kyoto Univ. 974 (1996) 30-42.

[10] Joseph, D. D., On the stability of the Boussinesq equations, Arch. Rat. Mech. Anal. 20 (1965) 59-71.

[11] Kawanago, T., Computer assisted proof to symmetry-breaking bifurcation phenomena in nonlinear vibration, Japan J. Indust, Appl. Math. 21 (2004) 75-108.

[12] Kim M., Nakao M. T., Watanabe Y. and Nishida T., A numerical verification method of bifurcating solutions for 3-dimensional Rayleigh-Bénard problems, Numerische Mathematik Vol.111 (2009) 389-406.

[13] Kirchgässner, K. and Kielhöfer, H., Stability and bifurcation in fluid dynamics, Rocky Mountain J. Math. 3 (1973) 275-318.

[14] Lorenz, E. N., Deterministic nonperiodic flow, J. Atmos. Sci. 20 (1963) 130-141.

[15] Nakao M. T., Watanabe Y., Yamamoto N., Nishida T. and M-N. Kim, Computer assisted proofs of bifurcating solutions for nonlinear heat convection problems, J. of Scientific Computing, Published online 2009 June.

[16] Nishida, T., Ikeda, T. and Yoshihara, H., Pattern formation of heat convection problems, Math. Model Numer. Simul. ed. by Miyoshi T., Springer (2001) 209-218.

[17] Nishida, T. and Teramoto, Y., On a linearized system arising in the study of Bénard-Marangoni convection, Proc. of Intern. Conf. on Navier-Stokes Equations and their Applications, RIMS Kokyuroku Bessatsu Vol.1, Kyoto Univ. (2007) 271-286.

[18] Nishida, T. and Teramoto, Y., Bifurcation theorem for the model system of Bénard-Marangoni convection, J. Math. Fluid Mechanics Vol.11 (2009) 383-406.

[19] Nishida, T. and Teramoto, Y., Pattern formations in heat-convection problems, Chinese Annals of Mathematics, Ser.B Vol.30 (2009) 769-784.

[20] Oberbeck, A., Über die Wärmeleitung der Flüssigkeiten bei der Berücksichtigung der Strömungen infolge von Temperaturdifferenzen, Annalen der Physik und Chemie 7 (1879) 271.

[21] Ogawa T., Hexagonal patterns of Bénard heat convection, RIMS Kokyuroku, Kyoto Univ. 1368 (2004).

[22] Rayleigh, L., On convection currents in a horizontal layer of fluid, when the higher temperature is on the under side, Phil. Mag. Ser. 6 32 (1916) 529-546.

[23] Urabe, M., Galerkin's procedure for nonlinear periodic systems. Arch. Rat. Mech. Anal. 20 (1965) 120-152.

[24] Velte, W., Stabilitätsverhalten und Verzweigung stationärer Lösungen der Navier-Stokesschen Gleichungen, Arch. Rat. Mech. Anal. 16 (1964) 97-125.

[25] Watanabe, Y., Yamamoto, N., Nakao, M. and Nishida, T., A numerical verification method for bifurcated solutions of Rayleigh-Bénard Problems, J. Math. Fluid Mechanics 6 (2004) 1-20.

[26] Yudovich, V. I., On the onset of convection, P. M. M. (J. Appl. Math. Mech.) 30 (1966) 1193-1199.